



PCCP

Two-dimensional self-assemblies of azobenzene derivatives: effects of methyl substitution of azobenzene core and alkyl chain length

Journal:	<i>Physical Chemistry Chemical Physics</i>
Manuscript ID	CP-ART-10-2022-005097.R1
Article Type:	Paper
Date Submitted by the Author:	25-Nov-2022
Complete List of Authors:	Kikkawa, Yoshihiro; National Institute of Advanced Industrial Science and Technology (AIST), Nagasaki, Mayumi; National Institute of Advanced Industrial Science and Technology (AIST) Norikane, Yasuo; National Institute of Advanced Industrial Science and Technology Tsukuba Center Tsukuba Central,

SCHOLARONE™
Manuscripts

ARTICLE

Two-dimensional self-assemblies of azobenzene derivatives: effects of methyl substitution of azobenzene core and alkyl chain length

Received 00th January 20xx,
Accepted 00th January 20xx

DOI: 10.1039/x0xx00000x

Yoshihiro Kikkawa,* Mayumi Nagasaki and Yasuo Norikane*

Elucidating the correlation between the molecular arrangement and physical properties of organic compounds is critical to facilitating the development of advanced functional materials. X-ray structural analyses are generally performed to clarify this relationship. Several attempts have been made to ascertain the links between three-dimensional (3D) crystals and their two-dimensional (2D) structures, which can be revealed by scanning tunnelling microscopy (STM) at the molecular level. Thus, 2D self-assemblies of a series of azobenzene derivatives were investigated in this study, and the effects of methyl substitution of the azobenzene core and alkyl chain length on the 2D molecular arrangements at the solid/liquid interface were revealed. Three types of azobenzene derivatives were prepared; these contained azobenzene (**Az**), 3-methyl azobenzene (**MAz**), or 3,3'-dimethyl azobenzene (**DAz**) as cores and alkyloxy chains of different lengths (C8–13) at their 4,4' positions. The 2D structures of the **Az** and **DAz** compounds were found to be modulated owing to the odd–even effect of the alkyl chains in a specific chain-length range; this effect was only weakly exhibited by the **MAz** compounds. This result suggests that only the methyl-group substitution of the azobenzene core significantly affected the 2D structures. The 2D structural features have been discussed in terms of molecular conformation, as well as their correlation with the photo-melting behaviour of the azobenzene derivatives, particularly the **MAz** compounds.

1. Introduction

Azobenzene is a fascinating molecular building block in the field of supramolecular chemistry because of its photo-switching ability. Photo-isomerisation routes such as *trans*-to-*cis* and *cis*-to-*trans* are generally induced by ultraviolet (UV) and visible light irradiation, respectively.¹ These topological changes of the azobenzene molecules enables not only molecular dynamic motion, but also macroscopic motion, such as actuation, bending, and crawling, which are expected for the applications in soft robotics and flexible devices.²

The photo-induced solid-to-liquid phase transition (photo-melting) of azobenzene based on photo-isomerization has been investigated in our previous studies.³ The photo-melting was first observed in a macrocyclic azobenzene.^{3a,b} Subsequently, a simple molecular modification involving the introduction of a methyl group at the 3-position of normal azobenzene derivatives was found to permit crystal-to-liquid phase transition.^{3c–f} In contrast, the derivatives with simple azobenzene and 3,3'-dimethyl azobenzene cores showed no photo-melting behaviour. Although the crystal structures of certain derivatives have been determined, the connections between the crystallographic information and photo-

melting behaviour remain unclear. Acquiring this insight can enable a deeper understanding of the photo-melting mechanisms, which will facilitate the development of advanced applications for such as reworkable adhesives, self-healing materials, and light energy storage materials.⁴

Typically, X-ray analyses have been performed to reveal the three-dimensional (3D) molecular arrangements of these compounds, which are known to influence their physical properties.⁵ Several recent studies have focused on clarifying the relationships between 3D structures and their two-dimensional (2D) assemblies, which can be revealed by scanning tunnelling microscopy (STM) at the molecular level.⁶ STM is particularly beneficial in terms of the preparation of a physisorbed monolayer, which is considerably simpler than growing single crystals for X-ray studies; simply placing the sample mixed with a poorly volatile solvent such as 1-phenyloctane onto highly oriented pyrolytic graphite (HOPG) enables the 2D self-assembly of molecules.⁷ Therefore, STM is effective for analysing the 2D structures of molecules with systematically modified chemical structures, such as alkyl chains.

Among the various intermolecular interactions, the dispersion force introduced by alkyl chains is considered relatively weak. However, alkyl chains often play an important role in ensuring adsorption onto the HOPG surface as well as in constructing the molecular arrangements in the self-assembled monolayer.⁸ The odd–even effect of alkyl chain lengths has been frequently documented in 2D and 3D systems; essentially, alkyl chains with odd or even numbers of carbons exhibit periodic changes in different characteristics including morphological and physical.⁹ This odd–even

National Institute of Advanced Industrial Science and Technology (AIST), Tsukuba Central 5, 1-1-1 Higashi, Tsukuba, Ibaraki 305-8565, Japan
E-mail: y.kikkawa@aist.go.jp, y.norikane@aist.go.jp

Electronic Supplementary Information (ESI) available: NMR data of azobenzene derivatives, and additional STM images. See DOI: 10.1039/x0xx00000x

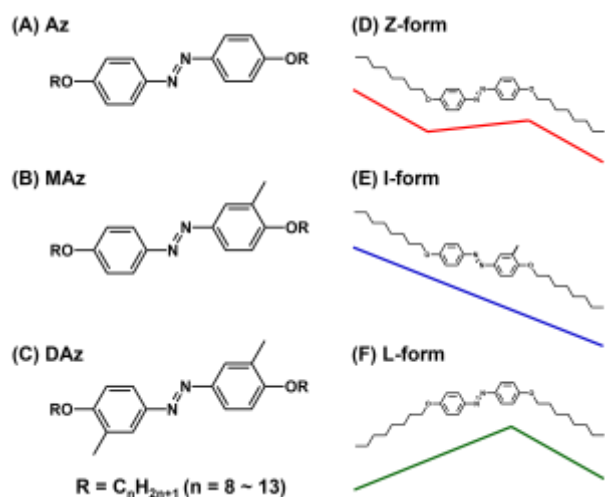


Fig. 1 Chemical structures of the investigated azobenzene derivatives containing (A) azobenzene (**Az**), (B) 3-methyl azobenzene (**MAz**), and (C) 3,3'-dimethyl azobenzene (**DAz**) cores and alkyloxy chains with different lengths at their 4,4' positions. The resulting derivatives are denoted as **AzCn**, **MAzCn**, and **DAzCn** (n [the number of carbon atoms in the alkyl chains] = 8–13). Panels (D)–(F) show the Z-, I-, and L-conformations of the compounds, respectively. The (D) and (F) panels show the Z- and L-forms of **Az** with C8 alkyl chains. (E) shows the I-form of **MAz** with C8 chains; this conformation is exhibited only by the **MAz** compounds (see text). The coloured lines are visual guides for the molecular conformations.

effect is believed to originate from the steric hindrance caused by the orientation of the terminal methyl group in the alkyl chain. Therefore, a small change in the number of $-\text{CH}_2-$ units can significantly affect the molecular arrangement, thereby yielding diverse 2D assemblies.^{9a} However, to our knowledge, systematic studies on the effects of methyl substitution of the azobenzene core and alkyl chain length on the 2D assemblies have not been reported.

Therefore, a series of azobenzene derivatives containing normal azobenzene (**Az**), 3-methyl azobenzene (**MAz**), and 3,3'-dimethyl azobenzene (**DAz**) as the core units along with alkyloxy chains of different lengths substituted at their 4,4' positions was prepared in this study. The resulting compounds are denoted as **AzCn**, **MAzCn**, and **DAzCn** ($n = 8$ –13; Fig. 1). These compounds were selected because their facile synthesis procedures enabled the production of differently modified compounds. The 2D structures of their molecules at the HOPG/1-phenyloctane interface were examined by STM, which assisted in clarifying the effects of the methyl substitution of the azobenzene core (molecular symmetry of azobenzene derivatives) and the alkyl chain length on the 2D molecular arrangement. Additionally, we discuss the correlation between the 2D structural features of these compounds and their photo-melting behaviour in the crystal phase was analysed.

2. Experimental

2.1 Synthesis of azobenzene derivatives

The azobenzene derivatives were prepared as previously reported.^{3c-f} Briefly, azobenzene skeletons were prepared by azo coupling of the corresponding aminophenol and phenol derivatives. The obtained azobenzene core units were

substituted with alkyl chains of different lengths via Williamson ether synthesis. Previously unreported compounds were characterised by ^1H NMR spectroscopy (Bruker Avance 400 NMR spectrometer) using tetramethylsilane as the standard (see Electronic Supplementary Information [ESI]).

2.2 STM observations

The azobenzene derivatives were dissolved in 1-phenyloctane at concentrations ranging from 1 to 100 mM. The shorter the alkyl chain length, the higher the concentration required for performing stable STM observations with sufficient resolution for analysing the molecular arrangements. For each compound, the variations in concentration did not affect the 2D structure. The 1-phenyloctane solutions containing the azobenzene derivatives were deposited individually on freshly cleaved HOPG (ZYB grade, MikroMasch). An STM tip was formed by mechanically cutting a Pt/Ir wire (90/10; ϕ 0.25 mm). The 2D structures at the HOPG/1-phenyloctane interface were examined by STM (Nanoscope IIIa, Digital Instruments). The HOPG lattice under the physisorbed monolayer was used as an internal standard to calibrate and correct the recorded STM images using the SPIP software (Image Metrology).

3. Results

3.1 Self-assembly of Az compounds

Figs. 2 and S1 show STM images of the 2D structures of **Az** molecules with different alkyl chain lengths ($n = 8$ –13) formed at the HOPG/1-phenyloctane interface. Considering the tunnelling current efficiency, the bright and dark regions in the STM images correspond to the azobenzene core and alkyl chains, respectively. A plausible molecular model is superimposed on the STM image in Fig. 2A. The **Az**-bearing octyl chains (denoted as **AzC8**; Fig. 2A) adopted the Z-conformation (Fig. 1D), and five **Az** cores were aligned parallel to form a cluster that was arranged as a parallelogram-shaped lattice (Fig. S1D). The C8 alkyl chains were interdigitated and aligned with

Table 1 Lattice constants of **Az** compounds measured from the STM images shown in Figs. 2 and S1. The parallelogram indicating the unit cell of each 2D structure is shown in Fig. S1.

Az	a (nm)	b (nm)	γ ($^\circ$)	Figures
C8	2.76 ± 0.10	3.43 ± 0.07	78 ± 2	2A, S1D
	1.11 ± 0.06	7.01 ± 0.10	85 ± 3	
C9	1.31 ± 0.05	1.71 ± 0.02	71 ± 1	2C, S1F
	1.32 ± 0.03	3.37 ± 0.07		
C11	1.30 ± 0.03	1.80 ± 0.15	74 ± 3	2E, S1K
	1.45 ± 0.08	3.76 ± 0.25		
C13-α	1.19 ± 0.03	2.08 ± 0.11	80 ± 2	2H, S1L

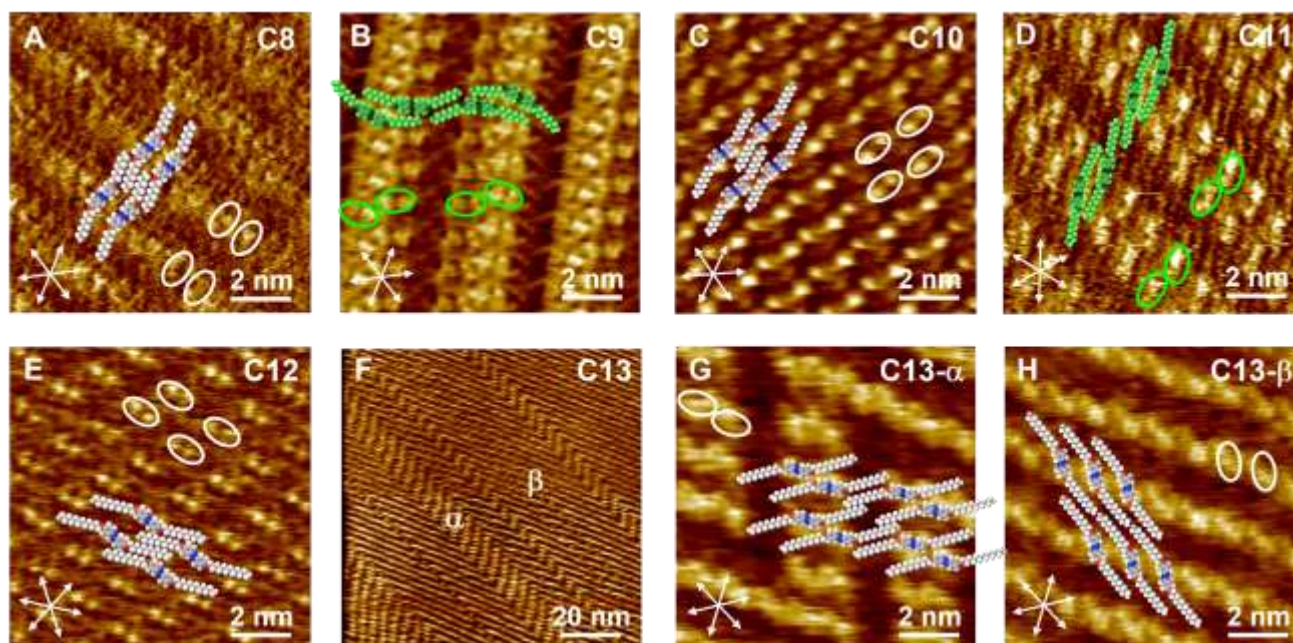


Fig. 2 STM images of **Az** molecules at the HOPG/1-phenyloctane interface. The white arrows in each image indicate the HOPG lattice directions. Panels (A)–(E) show STM images of **AzC8–12**, respectively, whereas panels (F)–(H) show those of **AzC13**. Panels (G) and (H) show enlarged STM images of the α and β domains in (F), respectively. The locations of the **Az** core unit are indicated by white (Z-form) and green ovals (L-form). Proposed molecular models are overlaid on the STM images; here, molecules in the L-form are highlighted in green. The lattice constants are listed in Table 1. Tunnelling conditions: (A) $I = 50$ pA, $V = -500$ mV; (B) $I = 50$ pA, $V = -817$ mV; (C) $I = 50$ pA, $V = -900$ mV; (D) $I = 25$ pA, $V = -1088$ mV; (E) $I = 25$ pA, $V = -500$ mV; (F–H) $I = 50$ pA, $V = -468$ mV.

one of the HOPG lattice directions. The lattice constants of **AzC8** are presented in Table 1.

Figs. 2B and 2D show the two-dimensional structures of **AzC9** and **AzC11** (odd number of carbons in the alkyl chain), respectively, whose proposed molecular models are superimposed onto the STM images. The locations of the azobenzene core units of **AzC9** and **AzC11** shifted from the side-by-side position, resulting in the core unit and alkyl chain being adjacent to each other. The combination of the core and alkyl chains formed columnar structures that were separated by the interdigitated alkyl chains. One of the alkyl chains in the dark-contrast regions was aligned along the HOPG axis, whereas the other one sandwiched by the cores was not. The 2D assemblies of both **AzC9** and **AzC11** comprised molecules in the L-form. With respect to **AzC10** and **AzC12** (even number of carbons in the alkyl chain; Figs. 2C and 2E, respectively), their cores were separately arranged (bright dots in the STM images), and the alkyl chains were interdigitated. A similar 2D structure of **AzC12** has been reported by De Schryver *et al.*¹⁰ Thus, columnar and separated structures were observed in the compounds containing an odd (**AzC9** and **AzC11**) and even (**AzC10** and **AzC12**) number of carbons, respectively. These results suggest that the **Az** compounds exhibited structural modulation for alkyl chain lengths of C9–C12.

In the case of **AzC13**, two types of randomly spaced 2D structures with different intervals between the bright regions were observed (α and β in Fig. 2F). Although the molecular arrangement could not be clearly resolved even in the enlarged images (Figs. 2G and 2H), plausible molecular models were generated based on the positions of the azobenzene core, assuming that the alkyl chains were oriented along a lattice direction of HOPG. In the α -domain (Fig. 2G), the azobenzene cores were positioned along their long axes, and the alkyl chains were partly interdigitated. The residual space was likely

occupied by the 1-phenyloctane (solvent) molecules.¹¹ In contrast, the azobenzene cores in the β -domain (Fig. 2H) were arranged as linear columns. The distance between the bright columns was too short to accommodate the alkyl chains perpendicular to the columnar direction; thus, the alkyl chains were likely configured in a head-to-head fashion. All lattice constants of the **Az** compounds are listed in Table 1.

3.2 Self-assembly of MAz compounds

The effect of methyl substitution at the 3-position in the azobenzene core on the 2D self-assembly was studied by STM at the HOPG/1-phenyloctane interface. Figs. 3 and S2 show STM images of **MAz** compounds with different alkyl chain lengths. In **MAzC8** (Fig. 3A), four bright bars formed a cluster that showed a stair-like arrangement; these were identified as the 3-methyl azobenzene

Table 2 Lattice constants of **MAz** compounds measured from the STM images shown in Figs. 3 and S2. The parallelogram indicating the unit cell of each 2D structure is shown in Fig. S2.

MAz	a (nm)	b (nm)	γ (°)	Figures
C8	2.16 ± 0.01	3.48 ± 0.06	83 ± 1	3A, S2D
	2.38 ± 0.03	3.32 ± 0.04	85 ± 1	
C9	2.40 ± 0.02	3.60 ± 0.04	78 ± 2	3C, S2F
	2.39 ± 0.06	5.04 ± 0.15	88 ± 2	
C10	2.61 ± 0.08	3.73 ± 0.09	72 ± 1	3E, S2K
	1.98 ± 0.05	5.24 ± 0.16	87 ± 2	
C11				3D, S2J
C12				3E, S2K
C13				3F, S2L

core, considering the tunnelling current efficiency. The two bars in the middle of each cluster were oriented diagonally to those on their sides. The dark lines that represented the alkyl chains were parallel to one of the HOPG axes, and all of them were interdigitated. Based on the alignment of the alkyl chains with one of the HOPG lattice directions, the two **MAzC8** molecules at the centre and ends of each cluster adopted the Z- and I-conformations, respectively. **MAzC9**, **MAzC10**, and **MAzC12** also exhibited similar stair-like structures (Figs. 3B, 3C, and 3E, respectively). **MAzC11** (Fig. 3D) had linear structures comprising two types of periodically aligned columns: one formed by alternate arrangement of the I-form and a pair of Z-form conformers, and the other consisting of only I-form molecules. In the case of **MAzC13** (Figs. 3F and S2L), two types of columns of **MAz** cores with different intervals were present. One of these columns comprised evenly arranged **MAz** cores with an interval (d_1) of 0.8 nm,

whereas the other was constructed by a pair of **MAz** cores with an interval (d_2) of 0.8 nm (Fig. S2L). The pairs of **MAz** molecules were periodically aligned with an interval (d_3) of 1.1 nm. In the neighbouring columns, the **MAz** cores were oriented in a herringbone pattern, that is, the core units were arranged in a zigzag fashion. Considering the different orientations and arrangements in each column (detailed discussion is presented later; also, see Fig. S4), they presumably included I- and Z-form molecules, which individually formed the columns. These results indicate that the 2D structures of **MAz** comprised both Z- and I-type conformers. The lattice constants of the **MAz** compounds are listed in Table 2.

3.3 Self-assembly of DAz compounds

Self-assembly of **DAz** compounds was investigated to clarify the effects of the dual substitution of methyl groups at the 3,3' positions of azobenzene on the formation of their 2D structures. Figs. 4 and S3 show STM images of **DAz** molecules at the HOPG/1-phenyloctane interface. **DAzC8** formed a dotted structure whose component molecules adopted a Z-type conformation with interdigitated alkyl chains. The **DAzC9–C13** compounds exhibited linear structures (Figs. S3B, S3C, and S3E–L). The higher-magnification images (Figs. 4B–4F) revealed that the linear structures comprised Z-type conformers with interdigitated alkyl chains. However, the orientations of the **DAz** core unit were dependent on the odd–even nature of the number of carbons in the alkyl chains, that is, the core units of **DAzC9**, **DAzC11**, and **DAzC13** arranged in a herringbone-like manner, whereas those of **DAzC10** and **DAzC12** were parallel aligned. These results suggest that the 2D structures of the **DAz** compounds were modulated for alkyl chain lengths of C9–C13. The lattice constants of the **DAz** compounds are listed in Table 3.

Table 3 Lattice constants of **DAz** compounds measured from the STM images in Figs. 4 and S3. The parallelogram indicating the unit cell of each 2D structure is shown in Fig. S3.

DAz	a (nm)	b (nm)	γ (°)	Figures
C8	1.26 ± 0.01	1.62 ± 0.02	70 ± 1	4A, S3D
C9	0.92 ± 0.01	4.30 ± 0.23	88 ± 2	4B, S3E
C10	0.95 ± 0.01	2.27 ± 0.06	83 ± 1	4C, S3F
C11	0.92 ± 0.01	5.01 ± 0.23	87 ± 3	4D, S3J
C12	0.92 ± 0.06	2.52 ± 0.04	85 ± 2	4E, S3K
C13	0.90 ± 0.04	5.36 ± 0.11	89 ± 1	4F, S3L

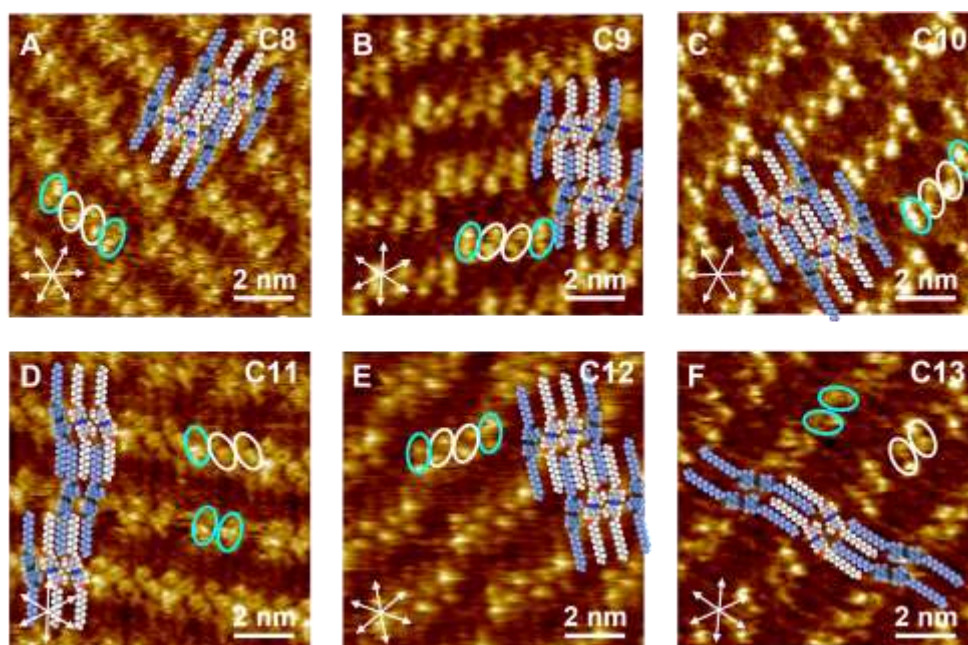


Fig. 3 STM images of **MAz** molecules at the HOPG/1-phenyloctane interface. The white arrows in each image indicate the HOPG lattice directions. Panels (A)–(F) show STM images of **MAzC8–13**, respectively. Proposed molecular models are overlaid on the STM images. The locations of the **MAz** core unit are indicated by white (Z-form) and cyan ovals (I-form). In the models, molecules in the I-form are highlighted in blue. The lattice constants are listed in Table 2. Tunnelling conditions: (A) $I = 50$ pA, $V = -800$ mV; (B) $I = 50$ pA, $V = -684$ mV; (C) $I = 25$ pA, $V = -584$ mV; (D) $I = 30$ pA, $V = -850$ mV; (E) $I = 30$ pA, $V = -340$ mV; (F) $I = 25$ pA, $V = -731$ mV.

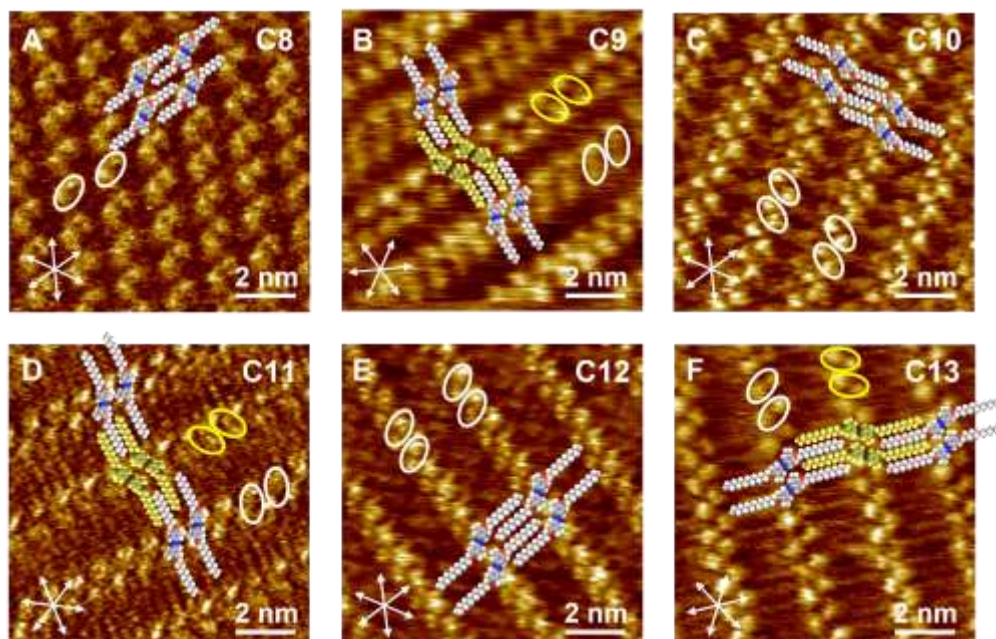


Fig. 4 STM images of **DAz** molecules at the HOPG/1-phenyloctane interface. The white arrows in each image indicate the HOPG lattice directions. Panels (A)–(F) show STM images of **DAzC8–13**, respectively. The locations of the **DAz** core unit are indicated by white and yellow ovals. Proposed molecular models are overlaid on the STM images. In panels (B), (D), and (F), the molecules with oppositely arranged **DAz** cores are highlighted in yellow; however, these have a Z-type conformation. The lattice constants are listed in Table 3. Tunnelling conditions: (A) $I = 25$ pA, $V = -778$ mV; (B) $I = 50$ pA, $V = -744$ mV; (C) $I = 50$ pA, $V = -1000$ mV; (D) $I = 25$ pA, $V = -566$ mV; (E) $I = 100$ pA, $V = -639$ mV; (F) $I = 25$ pA, $V = -809$ mV.

4. Discussion

4.1 The odd–even effect

The odd–even effect has previously been explained in terms of the direction of the terminal methyl group, and several compounds have been reported to exhibit diverse physical properties as well as 2D and 3D structures, depending on the odd–even nature of the alkyl chain carbons.⁹ In the **Az** and **DAz** compounds, 2D structural modulations were observed within specific alkyl-chain-length ranges. As shown in Figs. 2B–2E, columnar (**AzC9** and **AzC11**) and separated structures (**AzC10** and **AzC12**) were formed in the physisorbed monolayers. In the case of the **DAz** compounds (Fig. 4), the core units of **DAzC10** and **DAzC12** were oriented parallel to the neighbouring columns, whereas those of **DAzC9**, **DAzC11**, and **DAzC13** were arranged in a zigzag fashion. These results suggest the existence of the odd–even effect for **Az** and **DAz**, whose 2D structures changed in specific alkyl-chain-length ranges.

The **MAz** compounds, **MAzC8–10** and **MAzC12** showed stair-like structure, which had I-Z-Z-I sequences constructed by the I- and Z-form conformers. In contrast, the **MAzC11** and **MAzC13** compounds formed columnar structures. The columns for **MAzC11** were composed of I-Z-Z and I-I sequences, whereas those for **MAzC13** included separate I-I and Z-Z sequences. Despite the differences in the 2D structures between **MAzC8–10**, **12** and **MAzC11**, **13**, the **MAzC8–12** compounds have the same I-Z-Z sequence in their repeating units. The symmetric geometries of **Az** and **DAz** permitted simple packing of their structures with single-component Z-form molecules (partly the L-form ones for **AzC11** and **AzC13**), whereas full surface coverage by the **MAz** molecules was achieved by a mixture of two conformers (the I- and Z-forms) to compensate for their

asymmetry. Because of these two conformations of the **MAz** molecules, the alkyl-chain-end effect presumably became less significant, to the extent that only a weak odd–even effect could be observed for **MAzC10–13**. These results imply that the symmetric molecules, such as **Az** and **DAz**, exhibited a sharp odd–even effect, in contrast to the asymmetric **MAz**. Therefore, the symmetry of the molecules dictated the occurrence of the odd–even effect in the 2D structures of the investigated system.

4.2 Conformations of the building blocks

The 2D structures of **Az** and **DAz** essentially comprised molecules with a Z-type conformation, with certain exceptions such as **AzC9** and **AzC11**, which had L-form arrangements (Figs. 2 and 4). However, the **MAzC8–13** compounds had two conformations (the I- and Z-forms), indicating that the I-type conformation was allowed only for the **MAz** compounds. The crystal structures of **AzC6**, **MAzC6**, and **DAzC6** were revealed in our previous study^{3c} using X-ray analyses. In the (001) face of **MAzC6** and **DAzC6**, the positions of the methyl groups shift to circumvent their steric hindrance, that is, the neighbouring azobenzene core units become adjacent to each other for achieving close packing. In contrast, the azobenzene unit of **AzC6** viewed from the (101) face shifts from the face-to-face positioning and is sandwiched by the alkyl chains.

In the 2D assemblies (Fig. 2), most of the **Az** cores were offset from face-to-face positioning, and their close and parallel arrangements were interrupted by the alkyl chains, except for **AzC8**. However, the Z-form **MAz** and **DAz** cores (Figs. 3 and 4) were located parallel and adjacent to each other, similar to 3D crystals. In the **MAzC8–12** compounds (Figs. 3A–3E), the Z-type conformers were

present in a face-to-face configuration, with the protruded methyl groups being interlocked. The outer spaces of the Z-form components were occupied by the methyl group of the I-type conformer, and the alkyl chains were oriented parallel. Thus, combinations of the I- and Z-conformers were appropriately arranged to achieve close packing, due to the asymmetry of the **MAz** compounds.

The co-existence of the I- and Z-forms in the **MAz** series was further confirmed by measuring the angle (θ) between the orientations of the alkyl chain and core units. The DFT-optimised geometry of **MAzC10** indicated that the θ values for the I- and Z-forms were approximately 168° and 157°, respectively (Figs. S4A and S4B). The θ values measured from the STM images of **MAzC10**, **MAzC11**, and **MAzC13** (Figs. S4C-S4E) were almost identical to the DFT-calculated counterparts.

If the columnar structures in **MAzC13** were constructed by only one type of conformer, the intermolecular distances between its **MAz** cores would have been equal, as observed in the **DAzC9–13** molecules comprising Z- conformers with an interval of ~0.9 nm (lattice constants along the a -axis). However, one of the columns had evenly arranged intervals (d_1 in Fig. S2L), and the other comprised differently separated **MAz** cores (d_2 and d_3 in Fig. S2L). The measured angles and molecular intervals suggest that the columnar structures were constructed by different conformers; that is, one of the columns in **MAzC13** was formed by a pair of Z-type conformers, whereas the other comprised I-form molecules.

In situ and *ex situ* UV irradiation of the investigated azobenzene derivatives prevented the observation of 2D assemblies by STM; thus, the formation of the 2D assemblies with *cis* isomers could not be confirmed. The *trans* isomer was flat, whereas the *cis* isomer had a distorted geometry, which presumably impeded the STM observations from the viewpoint of planar adsorption onto the HOPG surface. Despite certain observations of 2D assemblies with *cis* isomers,¹² the *cis* isomers have been reported to be incapable of surviving long enough on the HOPG surface to permit STM-based visualisation, possibly because the HOPG surface catalyses the isomerisation from *cis* to *trans* conformations.¹³ Moreover, this rapid conversion from *cis* to *trans* isomers may disturb the stable formation of 2D assemblies in the investigated system.

4.3 Relationship between photo-melting behaviour and 2D assemblies

Azobenzene derivatives capable of switching between solid and liquid states upon exposure to UV light, that is, exhibiting photo-melting, were reported in our previous paper.³ Photo-melting was exhibited only by the **MAz** compounds, in contrast to the **Az** and **DAz** counterparts. Interestingly, the 2D assemblies of **MAz** specifically contained the I-type conformation in addition to the Z-type equivalent (Fig. 3), whereas those of **Az** and **DAz** primarily comprised the Z-form (Figs. 2 and 4). In certain cases, 2D systems have been reported to retain their intrinsic and characteristic molecular conformations in 3D crystals.⁶ These results suggest a possible correlation between the I-type conformation mixed with the Z-type conformers that enabled the construction of 2D assembly and the photo-melting behaviour of **MAz**.

MAz compounds with relatively short alkyl chains ($5 < n < 12$) were found in our previous study to exhibit faster photo-melting than those with long alkyl chains ($n > 12$).^{3e} The I- and Z-forms of the **MAzC8–12** molecules co-existed in their clusters (C8–10 and C12) or columns (C11). Despite that the 2D structure of **MAzC13** was also constructed by the I- and Z-form molecules, the molecules formed individual columns that were alternately arranged. Although **MAzC13** was photo-meltable, its rate was considerably lower than that of the other **MAz** with shorter alkyl chains. Therefore, the mechanism of the photo-melting behaviour of **MAz** with longer alkyl chains likely differs from that of the shorter-alkyl-chain compounds. Generally, 2D structures are not completely identical to 3D ones because of the presence of the substrate. Nevertheless, the correlation between the 2D assemblies and physical properties, such as photo-melting behaviour, was successfully estimated.

5. Conclusions

Azobenzene derivatives with different alkyl chain lengths (C8–C13) were prepared, and their 2D assemblies were studied by STM at the HOPG/1-phenyloctane interface. The core units of the azobenzene derivatives were normal azobenzene (**Az**), 3-methyl azobenzene (**MAz**), and 3,3'-dimethyl azobenzene (**DAz**). Modulation of the 2D structures through the odd–even effect was observed for the **AzC9–C12** and **DAzC9–C13** compounds in specific alkyl-chain-length ranges, however the effect was only weakly exhibited in the **MAzC10–13** compounds. This result suggests that the symmetry of the molecules influenced how the odd–even effect emerged.

The conformations of **Az** and **DAz** were essentially in the Z-form, except for **AzC9** and **AzC11**, which had I-type conformations. In contrast, the 2D structures of **MAz** comprised molecules with two conformations: I and Z. This result indicates that the I-type conformation was specific to the **MAz** compounds. Interestingly, photo-melting behaviour was exhibited only by the **MAz** compounds, implying a correlation between the 2D assemblies and physical properties such as photo-melting behaviour.

These results will permit the understanding of 2D assemblies from the viewpoints of the molecular symmetry introduced by methyl substitution of the molecular core unit as well as the alkyl-chain-length effect. Because a possible correlation between 2D assemblies and physical properties was suggested, this study is anticipated to facilitate the estimation of physical properties based on 2D assembly.

Conflicts of interest

There are no conflicts to declare.

Acknowledgements

This study was partly supported by the JST-Mirai Program (grant number JPMJMI21ED; Japan).

References

- 1 (a) H. M. D. Bandara and S. C. Burdette, *Chem. Soc. Rev.*, 2012, **41**, 1809–1825; (b) E. Merino and M. Ribagorda, *Beilstein J. Org. Chem.*, 2012, **8**, 1071–1090; (c) S. Lee, H. S. Kang and J.-K. Park, *Adv. Mater.*, 2012, **24**, 2069–2103.
- 2 (a) T. Taniguchi, T. Asahi and H. Koshima, *Crystals*, 2019, **9**, 437; (b) Y.-B. Wei, Q. Tang, C.-B. Gong and M. H.-W. Lam, *Anal. Chim. Acta*, 2015, **900**, 10–20; (b) H. Yu and T. Ikeda, *Adv. Mater.*, 2011, **23**, 2149–2180; (c) D. Dattler, G. Fuks, J. Heiser, E. Moulin, A. Perrot, X. Yao and N. Giuseppone, *Chem. Rev.*, 2020, **120**, 310–433; (d) L. Xu, F. Mou, H. Gong, M. Luo and J. Guan, *Chem. Soc. Rev.*, 2017, **46**, 6905–6926; (e) A. Goulet-Hanssens, F. Eisenreich and S. Hecht, *Adv. Mater.*, 2020, **32**, 1905966; (f) E. Uchida, R. Azumi and Y. Norikane, *Nat. Commun.*, 2015, **6**, 7310.
- 3 (a) Y. Norikane, Y. Hirai and M. Yoshida, *Chem. Commun.*, 2011, **47**, 1770–1772; (b) E. Uchida, K. Sakaki, Y. Nakamura, R. Azumi, Y. Hirai, H. Akiyama, M. Yoshida and Y. Norikane, *Chem. - Eur. J.*, 2013, **19**, 17391–17397; (c) Y. Norikane, E. Uchida, S. Tanaka, K. Fujiwara, E. Koyama, R. Azumi, H. Akiyama, H. Kihara and M. Yoshida, *Org. Lett.*, 2014, **16**, 5012–5015; (d) M. Hoshino, E. Uchida, Y. Norikane, R. Azumi, S. Nozawa, A. Tomita, T. Sato, S. Adachi and S. Koshihara, *J. Am. Chem. Soc.*, 2014, **136**, 9158–9164; (e) Y. Norikane, E. Uchida, S. Tanaka, K. Fujiwara, H. Nagai and H. Akiyama, *J. Photopolym. Sci. Technol.*, 2016, **29**, 149–157; (f) Y. Kikkawa, S. Tanaka and Y. Norikane, *RSC Adv.*, 2017, **7**, 55720–55724.
- 4 (a) T. Yamamoto, Y. Norikane and H. Akiyama, *Polym. J.*, 2018, **50**, 551–562; (b) L. Dong, Y. Feng, L. Wang and W. Feng, *Chem. Soc. Rev.*, 2018, **47**, 7339–7368.
- 5 (a) K. Yang, Z. Cai, M. Tyagi, M. Feygenson, J. C. Neuefeind, J. S. Moore and Y. Zhang, *Chem. Mater.*, 2016, **28**, 3227–3233; (b) Y. Zheng and P. Pan, *Prog. Polym. Sci.*, 2020, **109**, 101291; (c) O. Sato, *Nat. Chem.*, 2016, **8**, 644–656; (d) T. Iwata, H. Gan, A. Togo and Y. Fukata, *Polym. J.*, 2021, **53**, 221–238.
- 6 (a) R. Plamont, Y. Kikkawa, M. Takahashi, M. Kanesato, M. Giorgi, A. C. K. Shun, C. Roussel and T. S. Balaban, *Chem. - Eur. J.*, 2013, **19**, 11293–11300; (b) T. Hu, Y. Wang, M. Dong, J. Wu, X. Miao, Y. Hu and W. Deng, *J. Phys. Chem. C*, 2020, **124**, 1646–1654; (c) G. Raj, Y. Kikkawa, L. Catalano, R. Pasricha, Y. Norikane and P. Naumov, *ChemNanoMat*, 2020, **6**, 68–72; (d) A. Maranda-Niedbała, K. Krzyżewska, K. Kotwica, Ł. Skórka, J. Drapała, K. N. Jarzemska, M. Zagórska, A. Proń and R. Nowakowski, *Langmuir*, 2020, **36**, 15048–15063.
- 7 (a) J. Otsuki, *Coord. Chem. Rev.*, 2010, **254**, 2311–2341; (b) S. Uemura, R. Tanoue, N. Yilmaz, A. Ohira and M. Kunitake, *Materials*, 2010, **3**, 4252–4276; (c) Y. Kikkawa, *Polym. J.*, 2013, **45**, 255–260; (d) J. A. A. W. Elemans, *Adv. Funct. Mater.*, 2016, **26**, 8932–8951; (e) K. Iritani, K. Tahara, S. De Feyter and Y. Tobe, *Langmuir*, 2017, **33**, 4601–4618; (f) J. Teyssandier, K. S. Mali and S. De Feyter, *ChemistryOpen*, 2020, **9**, 225–241; (g) Y. Tobe, K. Tahara and S. De Feyter, *Chem. Commun.*, 2021, **57**, 962–977.
- 8 (a) Y. Wei, K. Kannappan, G. W. Flynn and M. B. Zimmt, *J. Am. Chem. Soc.*, 2004, **126**, 5318–5322; (b) K. Tahara, S. Furukawa, H. Uji-i, T. Uchino, T. Ichikawa, J. Zhang, W. Mamdouh, M. Sonoda, F. C. De Schryver, S. De Feyter and Y. Tobe, *J. Am. Chem. Soc.*, 2006, **128**, 16613–16625; (c) Y. Kikkawa, *Trans. Mat. Res. Soc. Jpn.*, 2014, **39**, 99–104; (d) Y. Kikkawa, E. Koyama, S. Tsuzuki, K. Fujiwara and M. Kanesato, *Langmuir*, 2010, **26**, 3376–3381; (e) Y. Kikkawa, S. Tsuzuki, A. Kashiwada and K. Hiratani, *Colloids Surf., A*, 2018, **537**, 580–590; (f) Y. Fang, M. Cibian, G. S. Hanan, D. F. Perepichka, S. De Feyter, L. A. Cuccia and O. Ivashenko, *Nanoscale*, 2018, **10**, 14993–15002; (g) M. Maeda, R. Nakayama, S. De Feyter, Y. Tobe and K. Tahara, *Chem. Sci.*, 2020, **11**, 9254–9261.
- 9 (a) F. Tao and S. L. Bernasek, *Chem. Rev.*, 2007, **107**, 1408–1453; (b) L. Xu, X. Miao, B. Zha, K. Miao and W. Deng, *J. Phys. Chem. C*, 2013, **117**, 12707–12714; (c) Y. Xue, M. K. Kim, T. Pašková and M. B. Zimmt, *J. Phys. Chem. B*, 2013, **117**, 15856–15865; (d) E. Ghijssens, O. Ivashenko, K. Tahara, H. Yamaga, S. Itano, T. Balandina, Y. Tobe and S. De Feyter, *ACS Nano*, 2013, **7**, 8031–8042; (e) E. Badea, B. Nowicka and G. Della Gatta, *J. Chem. Thermodyn.*, 2014, **68**, 90–97; (f) Z. Wang, J. Chen, S. Oyola-Reynoso and M. Thuo, *Coatings*, 2015, **5**, 1034–1056; (g) Y. Hu, K. Miao, B. Zha, X. Miao, L. Xu and W. Deng, *RSC Adv.*, 2015, **5**, 93337–93346; (h) Y. Hu, K. Miao, B. Zha, L. Xu, X. Miao, and W. Deng, *Phys. Chem. Chem. Phys.*, 2016, **18**, 624–634; (i) Y. Hu, K. Miao, L. Xu, B. Zha, X. Miao and W. Deng, *RSC Adv.*, 2017, **7**, 32391–35398.
- 10 P. C. M. Grim, P. Vanoppen, M. Rücker, S. De Feyter, S. Valiyaveetil, G. Moessner, K. Müllen, and F. C. De Schryver, *J. Vac. Sci. Technol. B: Microelectron. Nanometer Struct.--Process., Meas., Phenom.*, 1997, **15**, 1419.
- 11 (a) Y. Yang and C. Wang, *Curr. Opin. Colloid Interface Sci.*, 2009, **14**, 135–147; (b) O. Ochs, M. Hocke, S. Spitzer, W. M. Heckl, N. Martsinovich and M. Lackinger, *Chem. Mater.*, 2020, **32**, 5057–5065; (c) Y. Kikkawa, M. Nagasaki, E. Koyama, S. Tsuzuki and K. Hiratani, *Chem. Commun.*, 2019, **55**, 3955–3958.
- 12 (a) P. Vanoppen, P. C. M. Grim, M. Rücker, S. De Feyter, G. Moessner, S. Valiyaveetil, K. Müllen and F. C. De Schryver, *J. Phys. Chem.*, 1996, **100**, 19636–19641; (b) C. L. Feng, Y. Zhang, J. Jin, Y. Song, L. Xie, G. Qu, L. Jiang and D. Zhu, *Surf. Sci.*, 2002, **513**, 111–118; (c) M. E. Garah, E. Borré, A. Ciesielski, A. Dianat, R. Gutierrez, G. Cuniberti, S. Bellemin-Lapponnaz, M. Mauro and P. Samorì, *Small*, 2017, **13**, 1701790.
- 13 J. Zeitouny, C. Aurisicchio, D. Bonifazi, R. De Zorzi, S. Geremia, M. Bonini, C.-A. Palma, P. Samorì, A. Listorti, A. Belbakra and N. Armaroli, *J. Mater. Chem.*, 2009, **19**, 4715–4724.